American Journal of Optics and Photonics
2022; 10(2): 10-15
http://www.sciencepublishinggroup.com/j/ajop
doi: 10.11648/j.ajop.20221002.11
ISSN: 2330-8486 (Print); ISSN: 2330-8494 (Online)

Optically-Pumped Edge-Emitting Semiconductor Laser Using Coupled Ridge-Waveguide Structure

Nithin Vogirala*, Mangalpady Rajaram Shenoy

Department of Physics, Indian Institute of Technology Delhi, New Delhi, India

Email address:

v.nithin@physics.iitd.ac.in (Nithin Vogirala), mrshenoy@physics.iitd.ac.in (Mangalpady Rajaram Shenoy)

*Corresponding author

To cite this article:

Nithin Vogirala, Mangalpady Rajaram Shenoy. Optically-Pumped Edge-Emitting Semiconductor Laser Using Coupled Ridge-Waveguide Structure. *American Journal of Optics and Photonics*. Vol. 10, No. 2, 2022, pp. 10-15. doi: 10.11648/j.ajop.20221002.11

Received: October 10, 2022; **Accepted**: October 28, 2022; **Published**: November 4, 2022

Abstract: In this paper, the authors propose an integrated design of an in-plane optically-pumped edge-emitting ridge-waveguide semiconductor laser, without any bulk components. The optical pump radiation is transferred to the active region of the laser through coupling from the adjacent transparent waveguide. The laser device is based on $In_{1-x}Ga_xAs_yP_{1-y}$/InP heterojunction, with a pump at 1310 nm wavelength and lasing around 1550 nm. The proposed scheme enables optical-to-optical signal control, in place of the current controlled signal in an electrically-biased semiconductor laser. Since the structure doesn't require any p-n junctions, a high-quality active material with minimum doping can be employed. In order to simulate the steady-state characteristics of an optically-pumped semiconductor laser, the well-established Connelly's model for semiconductor optical amplifiers (SOAs) is suitably modified. The validity of the model for semiconductor lasers is established by showing that the evolution of simulated longitudinal modes conforms with the prediction of laser theory. For the chosen device parameters, under optimum operating conditions, the threshold pump power is found to be ≈ 70 mW along with a high pump power conversion efficiency (i.e output laser power/input pump power) of 61%. The proposed all-optically pumped semiconductor laser could be in the form of a 2-port fiber pig-tailed integrated optical device, without the need for any bias current.

Keywords: Optical Pumping, Semiconductor Lasers, Integrated Optics, Waveguide Coupling

1. Introduction

Conventionally, semiconductor lasers are p-n junction based heterostructure devices which are electrically pumped to achieve the lasing operation. Recently, there have been several reports on the study of optical pumping in semiconductor lasers and amplifiers. Research in optical pumping of VCSELs has made considerable progress, and very high output powers have been reported [1-5]. Several schemes have also been reported on optical pumping of edge-emitting semiconductor lasers [6-10]. Almost all the schemes employ optical pumping by irradiation through the sides or from the top of the active region along its length. Due to a very small thickness of the active layer (<1 μm), only a fraction of the pump power is absorbed in generating carriers, which results in a low pump-power conversion efficiency of the device. To increase the absorbed pump power, high reflectivity mirrors are employed at the sides to reflect the unutilized pump power back into the active region [6, 7]. However, this substantially increases the device complexity. Toikkanen et al [8] employed a waveguide structure with a relatively large width of the active region, to allow for uniform optical illumination through a cylindrical lens; however, this leads to multiple transverse modes of the laser, which is not desirable in many applications. Moreover, due to the requirement of bulk components in the arrangement for light illumination, the scheme of optical pumping through external illumination is not compatible with photonic integrated circuit (PIC) [11].

In our earlier communication, an improved optical pumping scheme for an SOA based on the coupled ridge

waveguide structure was proposed [12]. The pumping scheme enabled a single transverse-mode operation and low polarization dependence of the device. However, in implementing the proposed optical pumping scheme in SOA, it would face a fabrication challenge of inputting two separate fiber pigtails (for the input signal and the input pump) at the input end of the SOA. It would require fanning-in of the fiber pigtails, which would increase the length and the complexity of the device. In this paper, the authors propose an integrated design of an optically-pumped edge-emitting semiconductor laser, in which the coupled-waveguide optical pumping scheme is simpler to implement. In the proposed device, due to efficient ultilization of pump power, a higher pump-power conversion efficiency is obtained. Since the laser structure doesn't require any p-n junctions, high-purity semiconductor materials with minimum dopants/impurity can be employed to minimize the defects and the intrinsic losses. In Section 2, the design of the proposed device is presented. The numerical model for the simulation is outlined in Section 3, and the simulation results on the performance characteristics of the proposed device are presented in Section 4.

2. Scheme of the Optically-Pumped Edge-Emitting Semiconductor Laser

Figure 1 shows a schematic of the proposed device. A ridge-waveguide directional coupler comprising of the pump waveguide and the active waveguide is considered. The pump radiation is injected into the input facet of the pump-waveguide through a fiber pigtail. The pump couples to the active waveguide, all along its length, through evanescent field interaction. The coupled pump power is absorbed in the active waveguide, and thus the carriers are generated throughout the active waveguide. When the carrier density is above the threshold, then lasing action takes place in the active waveguide, and the laser output is obtained through a separate fiber pigtail at the output facet. Unlike the case of optically-pumped SOA [12], the fiber pigtail can be simply connected to the input end without requiring any fanning-in. Thus, the proposed device will be a standalone 2-port integrated optical laser.

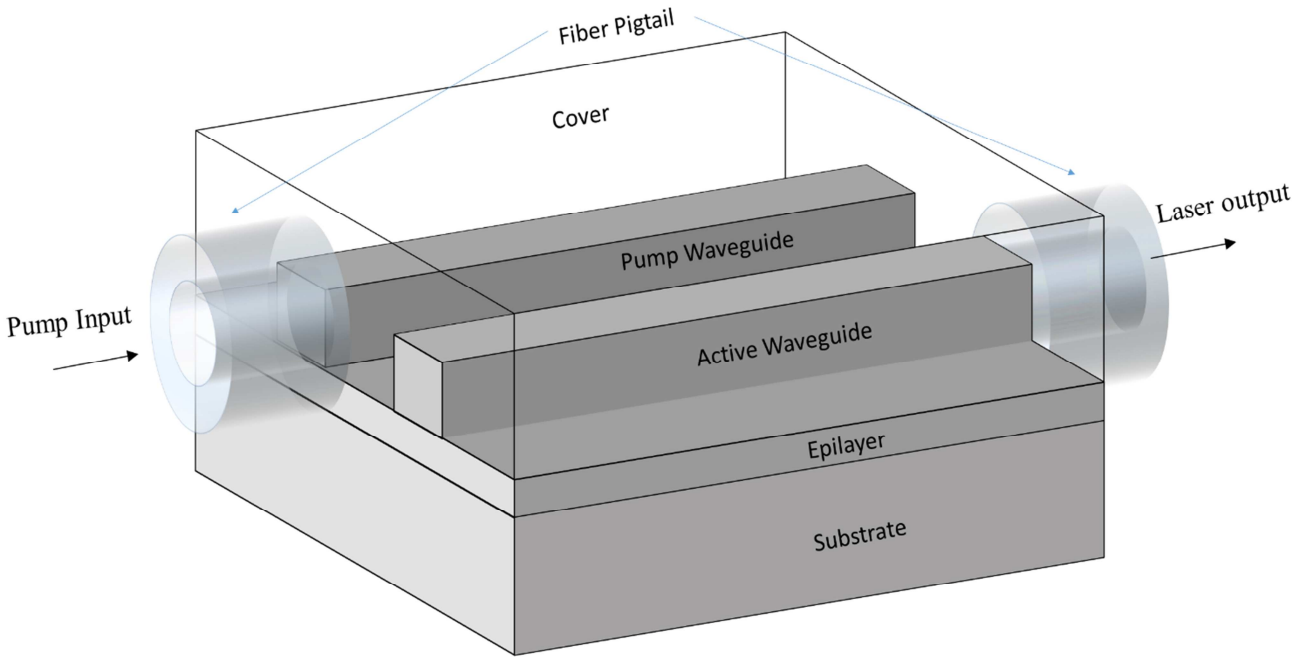

Figure 1. *Schematic of the proposed optically-pumped edge-emitting semiconductor laser in which pumping takes place through evanescent wave coupling in the ridge-waveguide coupler.*

The proposed device is based on lattice-matched $In_{1-x}Ga_xAs_yP_{1-y}$/InP material system (x = 0.46y) [12]. The pump is at a wavelength of 1310 nm. The lasing wavelength is around 1550 nm. The pump waveguide is transparent to the pump. The waveguide parameters are chosen such that both pump waveguide and active waveguide supports only the fundamental transverse mode. The coupled-waveguide structure is designed to ensure that the pump power is uniformly available in the length of the active waveguide (see Section 4). Figure 2 shows the materials and the dimensions of the waveguides in the design of the proposed device. The length of the device is chosen to be 500 μm. The list of waveguide parameters used in the proposed device are given in Table 1.

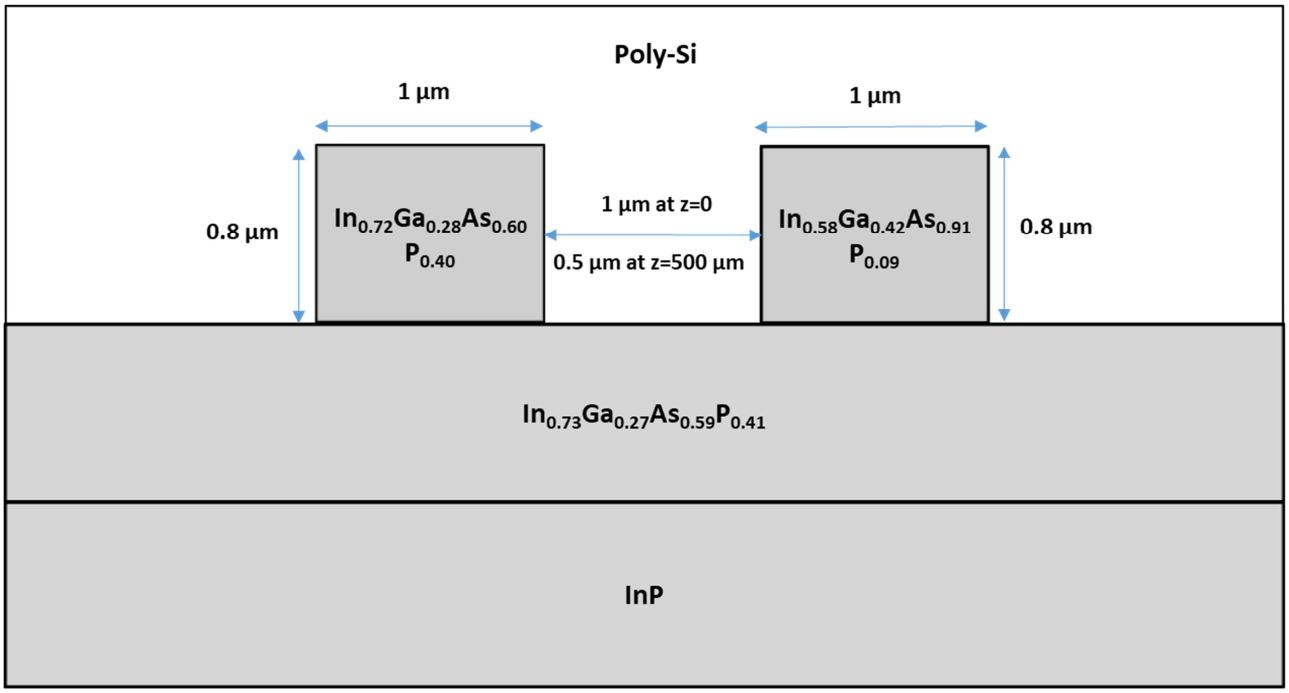

Figure 2. *The transverse cross section of the coupled-waveguide structure showing the materials and the dimension involved. The separation between the waveguides is linearly decreased from 1 µm at z=0 to 0.5 µm at z= 500 µm.*

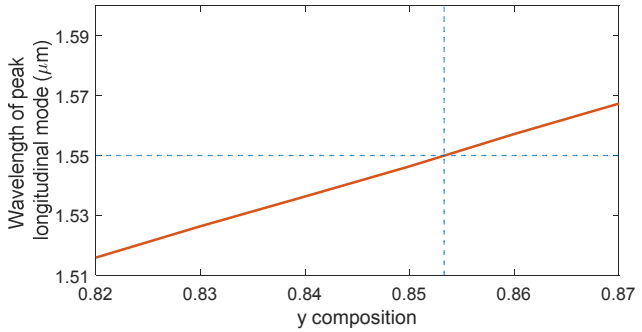

Figure 3. *Plot of wavelength corresponding to the peak longitudinal mode at the laser output with y composition.*

Table 1. *List of the waveguide parameters used in the design of the proposed device.*

Parameter	Value
Length (L)	500 µm
Active waveguide's width (w_A)	1 µm
Active waveguide's thickness (t_A)	0.8 µm
Pump waveguide's width (w_P)	1 µm
Pump waveguide's thickness (t_P)	0.8 µm
Epilayer thickness	4 µm
Inter-waveguide separation (linearly decreasing)	1 µm (at z = 0) 0.5 µm (at z = L)

The material composition of the core of the active waveguide has to be chosen such that the peak longitudinal mode in the laser output of the simulated device is at a wavelength of 1550 nm; this corresponds to y = 0.853 (see Figure 3). At this composition of $In_{1-x}Ga_xAs_yP_{1-y}$, the absorption coefficient at 1310 nm is ≈ 5.4×10^5 m^{-1}. Thus, the composition of $In_{1-x}Ga_xAs_yP_{1-y}$ with y = 0.853 for the core of the active waveguide is very favourable for the laser operation. The plot in Figure 3 has been obtained by using the numerical model outlined later in Section 3.

3. Numerical Modelling of the Laser

The Connelly's model [13] of SOA is modified to simulate the output characteristics of the proposed optically-pumped semiconductor laser. The process starts from the spontaneously generated noise in the active waveguide to the build-up of amplified spontaneous emission (ASE) at the longitudinal modes and finally to lasing at the peak longitudinal mode(s) due to the reflection from the ends. The spontaneous emissions and the stimulated emissions take place because of the recombination of the carriers. The carriers are generated due to the absorption of pump throughout the length of the active waveguide. The active waveguide has been divided into a suitable number of sections of length Δz. The carrier density N in the i^{th} section at time t is evaluated through the following carrier density rate equation [13]:

$$\frac{dN_i(z,t)}{dt} = \frac{\Gamma_P}{tw}\left\{\frac{\lambda_P\,\alpha_P(N_i,\lambda_P)}{hc}P_P(z,t)\right\} - R - \frac{2\Gamma_{ASE}}{tw} \times \left\{\sum_{j=0}^{N_m-1}\frac{\lambda_j\, g_m(N_i,\lambda_j)}{hc}K_j\left[P_{ASE}^{+}(N(z)) + P_{ASE}^{-}(N(z))\right]\right\} \quad (1)$$

where P_P represents the pump power; P_{ASE}^{+} and P_{ASE}^{-} represent the power of the forward and backward propagating ASE, respectively; K_j is the filter factor, which represents the fraction of spontaneously emitted photons that gets coupled into the guided mode; R is the total recombination rate, which is the sum of radiative and non-radiative recombination rates;

Γ_P and Γ_{ASE} are the optical confinement factors for the pump and ASE, respectively.

In (1) the term representing the carrier generation due to the current in [13] is replaced with the term representing the carrier generation due to the absorption of the optical pump (cf. the first term on the RHS of (1)).

The material gain (or absorption) coefficient g_m (or α_m) in the $In_{1-x}Ga_xAs_yP_{1-y}$ active region is given by [13]:

$$g_m(N,\lambda) = \frac{\lambda^2}{4\sqrt{2}\,\pi^{\frac{3}{2}} n_1^2 \tau}\left(\frac{4\pi m_e m_{hh}}{h(m_e+m_{hh})}\right)^{\frac{3}{2}} \times \sqrt{\frac{c}{\lambda} - \frac{E_g(N)}{h}}\left(f_c(\lambda) - f_v(\lambda)\right) \quad (2)$$

The ASE build-up is significant at the resonance frequency of the laser cavity. The resonant frequencies are given by:

$$\lambda_j = \frac{c}{\nu_j} \text{ with } \nu_j = \frac{E_{g0}}{h} + \Delta\nu_c + jK_m\Delta\nu_m \quad (3)$$

$$j = 0 \ldots N_m - 1$$

where E_{g0} is the bandgap energy of the active material, $\Delta\nu_c$ is the frequency offset to match ν_0 to resonance, $\Delta\nu_m$ is the free spectral range, N_m and K_m are integers which depend on the gain bandwidth and required accuracy for the numerical simulation.

The evolution of the ASE in the active waveguide is given by the traveling wave equation [13]:

$$\frac{dP_{ASE}(z)}{dz} = (\Gamma g_m(N,\lambda_S) - \alpha)P_{ASE}(z) \quad (4)$$

The pump power (P_P) in each section of the active waveguide comprises the propagating pump power from the previous section plus the power coupled from the pump waveguide into that section. To estimate the pump power in any particular section of the active waveguide ($P_P^{AW}(z)$), the corresponding traveling wave equation for the pump is used [14]:

$$\frac{dP_P^{AW}(z)}{dz} = (\Gamma g_m(N,\lambda_P) - \alpha)P_P^{AW}(z) \quad (5)$$

The pump power coupled from the pump waveguide ($P_P^{CW}(i)$) into that section is then added, to obtain the net pump power in the particular section of the active waveguide [14]:

$$P_P(z+\Delta z) = P_P^{AW}(z) + P_P^{CW}(i) \quad (6)$$

where $P_P^{CW}(i)$ refers to pump power added to the i^{th} segment and is determined by using the OptiBPM software. The active waveguide has cleaved-end facets, and therefore the end-facet reflectivity is taken as 32% each.

4. Results and Discussion

This section presents the simulation results on the performance characteristics of an InGaAsP/InP based edge-emitting semiconductor laser, which is pumped by an optical source at 1310 nm wavelength. In our analysis, the optically pumped semiconductor laser is considered as a polarization independent device. This is because the optical confinement factor for the TE and TM modes are almost identical because of the near-symmetric cross section of the active-waveguide (1 µm x 0.8 µm).

Figure 4 shows the evolution of forward-propagating lasing mode power, the backward-propagating lasing mode power and the pump power in the active waveguide along the length of the optically-pumped laser at the steady-state for an input pump power of 100 mW. Due to the initial coupling of pump power from the pump waveguide to the active waveguide, there is sharp rise in the pump power from z = 0 to z ≈ 70 µm. In the latter portion, the pump power is almost uniformly available throughout the active waveguide. Accordingly, the longitudinal carrier density profile is also mostly uniform along the active waveguide (see the inset figure). The power profile of the forward- and backward-propagating lasing mode follows the longitudinal distribution of the carrier density. Higher the carrier density, higher will be the rate of stimulated emissions; therefore, the power in the lasing mode also increases as it propagates along the length of the active waveguide. The near symmetric nature of forward- and backward-propagating lasing mode is consistent with the prediction of laser theory [11, 15].

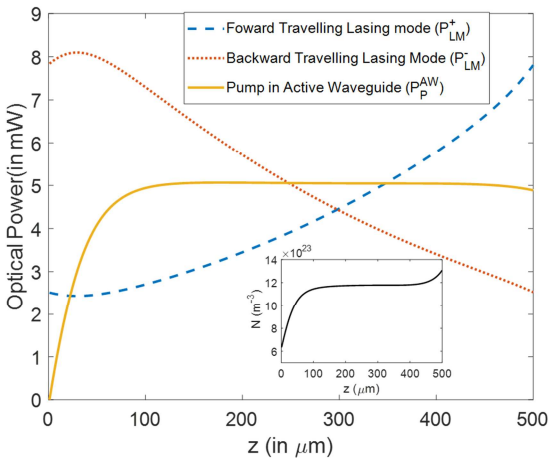

Figure 4. *The steady-state power profiles of the forward-propagating lasing mode (P^+_{LW}), the backward-propagating lasing mode (P^-_{LW}) and the pump power (P_P^{AW}) along the active waveguide of the optically-pumped for an input pump power of 100 mW. The inset figure shows the carrier density distribution along the active waveguide.*

Figure 5 shows the distribution of power among the different longitudinal modes at the laser output. Just below the threshold (Figure 5(a)), the laser output is very small, and the power is distributed almost equally over the various cavity modes. Just above the threshold (Figure 5(b)), the output power increases, and the power distribution among the modes follows the gain profile. As the pump power is increased further (Figure 5(c) and 5(d)), the output power increases further and major fraction of the power gets distributed into few longitudinal modes centered around the peak gain

coefficient (λ ≈ 1550 nm, mode no. 10). This evolution and distribution of laser power among the longitudinal modes with increasing pump power is consistent with that observed in the case of a conventional electrically biased laser.

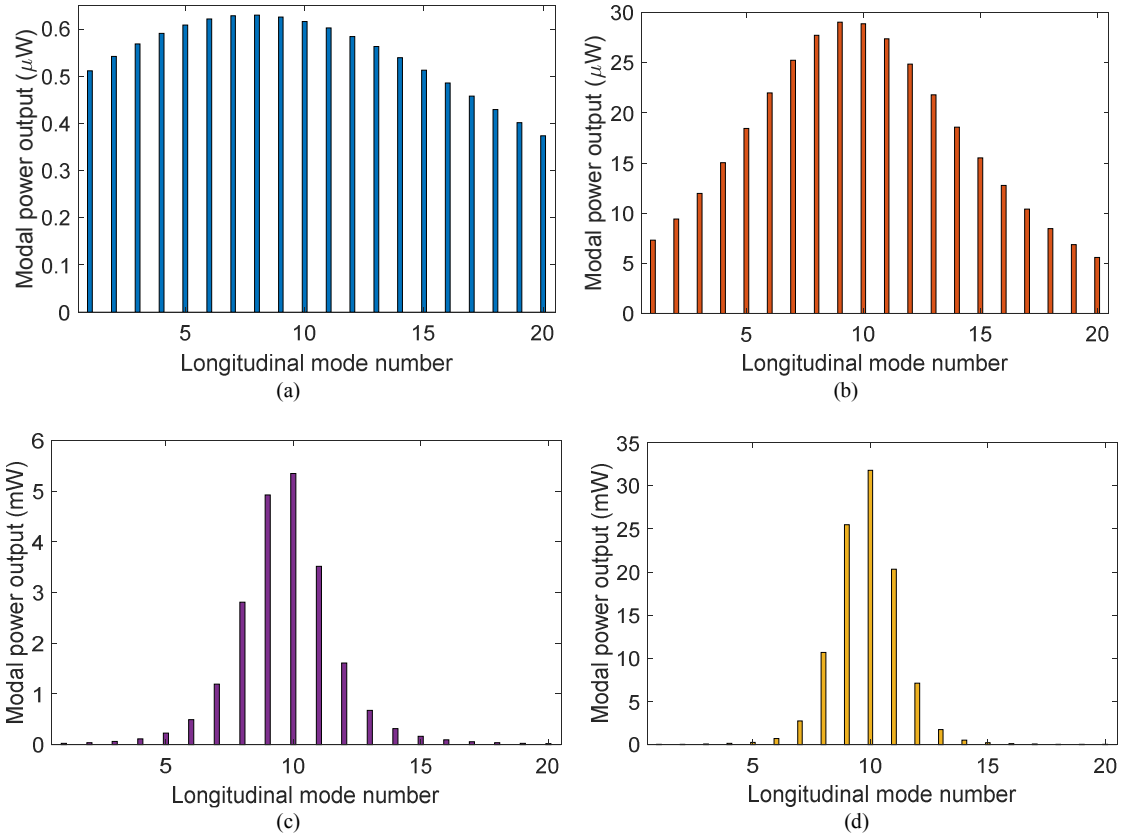

Figure 5. *The evolution and distribution of laser output power among the longitudinal modes of the laser when the input pump power is (a) Ppump = 68 mW (just below threshold), (b) Ppump =72 mW (just above the threshold), (c) Ppump =100 mW (well above the threshold) and (d) Ppump =200 mW (far above the threshold).*

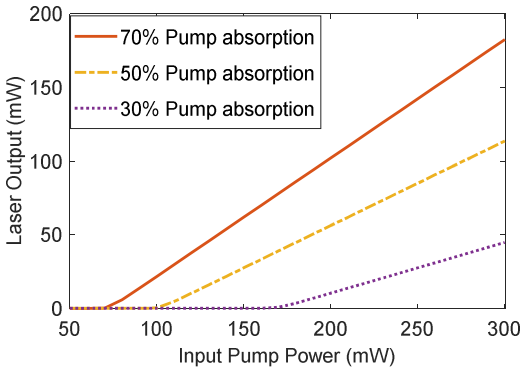

Figure 6. *Variation of output power with the input pump power for three different cases of pump power absorption.*

Figure 6 shows the variation of the output power of the laser with the input pump power for three different magnitudes of pump power absorption (30%, 50%, and 70%); correspondingly, the pump power conversion efficiencies are estimated to be 15%, 38%, and 61%; the corresponding threshold pump powers are 170 mW, 100 mW, and 70 mW, respectively. In our design, 70% of pump power is absorbed (α = -5.65×105 m-1). As the absorbed pump power increases, the pump conversion efficiency approaches the 'quantum defect' $(1-(1310/1550) = 15.5\%)$. Also, as expected, threshold pump power decreases with higher pump power absorption.

In our simulations, it is found that the length of the device is one of the important parameters to the device performance. By taking a smaller device length (say 300 μm), the pump power transfer efficiency is very less because the length over which the coupling takes place is short. Moreover, there would be a large number of lasing longitudinal modes. On the other hand, by taking a longer device length (say 700 μm), the threshold pump power becomes very large, although there would be lesser number of lasing longitudinal modes. Therefore, keeping in view of the optimum threshold pump power and the number of lasing modes, a device length of 500 μm is chosen.

Optical pumping with a high pump-power conversion efficiency could be realized due to the optimum pump power injection into the active waveguide by employing the coupled-waveguide configuration. Also, the use of such configuration for pumping makes the device compact, and could be integrated into PICs. Further, use of high radiance LEDs as the pump source could be explored as a cost-effective alternative.

We may mention that ridge waveguides and coupled ridge waveguide structures are routinely fabricated in integrated

optics; however, in the proposed design, the two coupled ridge waveguides have their core layers made up of slightly different compositions of the alloy $In_{1-x}Ga_xAs_yP_{1-y}$, and it would require selective lithographic procedure (including growth and etching) for the core layers of the ridge. This would necessitate two or three additional steps in the fabrication. All other layers comprise of the same material and thickness for both the waveguides. It may also be noted that the proposed device does not require the fabrication step of metallization. The next step would be to fabricate the proposed device.

5. Conclusion

A novel device configuration to realize an efficient optically-pumped edge-emitting semiconductor laser through transverse waveguide-coupling of the optical pump is proposed. By an optimum choice of materials and design of the coupled-waveguide structure, the proposed laser can have a single transverse-mode operation with low polarization dependence. Optical pumping provides the desirable optical-to-optical laser output control, and could have potential applications in all-optical signal processing. For typical values of the various device parameters, our numerical results show that a high pump power conversion efficiency (61%) with a threshold pump power of 70 mW could be achieved. A practical standalone laser may be realized in the form of a 2-port fiber pigtailed device, with one fiber supplying the pump beam and the other bringing the laser output.

References

[1] M. Guina, A. Rantamäki, and A. Härkönen, “Optically pumped VECSELs: review of technology and progress,” J Phys D Appl Phys, vol. 50, no. 38, 2017, doi: 10.1088/1361-6463/aa7bfd.

[2] G. Hou et al., “Near-diffraction-limited semiconductor disk lasers,” Opt Commun, vol. 449, pp. 39–44, 2019, doi: 10.1016/j.optcom.2019.05.035.

[3] Z. Yang, A. R. Albrecht, J. G. Cederberg, and M. Sheik-Bahae, “Optically pumped DBR-free semiconductor disk lasers,” Opt Express, vol. 23, no. 26, pp. 33164–33169, 2015, doi: 10.1364/OE.23.033164.

[4] Coherent, “Optically Pumped Semiconductor Lasers.” [Online]. Available: https://content.coherent.com/legacy-assets/pdf/Optically-Pumped-Semiconductor-Laser-Brochure.pdf

[5] P. Qiu et al., “Realization of single-transverse-mode VCSELs incorporating a built-in index guide,” Opt Commun, vol. 504, 2022, doi: 10.1016/j.optcom.2021.127450.

[6] R. D. Clayton and B. Reid, “Monolithically integrated optically-pumped edge emitting semiconductor laser”

[7] S. G. Anikitchev, H. Zhou, and R. R. Austin, “Optically pumped edge-emitting semiconductor laser”

[8] L. Toikkanen et al., “Optically Pumped Edge-Emitting GaAs-Based Laser With Direct Orange Emission,” IEEE Photonics Technology Letters, vol. 26, no. 4, pp. 384–386, 2014, doi: 10.1109/lpt.2013.2294726.

[9] C. Ruan et al., “Gain-coupled 770 nm DFB semiconductor laser based on surface grating,” Opt Commun, vol. 479, 2021, doi: 10.1016/j.optcom.2020.126377.

[10] I. Panyaev, I. Zolotovskii, and D. Sannikov, “Laser generation and amplification of TE and TM modes in a semiconductor optical GaAs waveguide with distributed feedback generated by a space charge wave,” Opt Commun, vol. 459, 2020, doi: 10.1016/j.optcom.2019.125026.

[11] G. P. Agrawal and N. K. Dutta, Semiconductor Lasers. US: Springer, 1995.

[12] N. Vogirala, M. Shenoy, and Y. Kumar, “Efficient Optically-Pumped Semiconductor Optical Amplifier in a Coupled-Waveguide Configuration: A Novel Proposal,” IEEE Photonics J, vol. 13, no. 6, pp. 1–6, 2021, doi: 10.1109/jphot.2021.3120846.

[13] M. J. Connelly, “Wideband semiconductor optical amplifier steady-state numerical model,” IEEE J Quantum Electron, vol. 37, no. 3, pp. 439–447, 2001, doi: 10.1109/3.910455.

[14] V. Nithin, Y. Kumar, and M. R. Shenoy, “Novel scheme of assist-light injection through waveguide coupling in a semiconductor optical amplifier for fast gain recovery,” Opt Commun, vol. 359, pp. 419–425, 2016, doi: https://doi.org/10.1016/j.optcom.2015.09.094.

[15] D. J. Klotzkin, Introduction to semiconductor lasers for optical communications. Springer, 2020.